Inorganic Chemistry

Article

pubs.acs.org/IC

Effects of Metal Coordination on the π-System of the 2,5-Bis-{(pyrrolidino)-methyl}-pyrrole Pincer Ligand

Christian Maaß,[†] Diego M. Andrada,[‡,§] Ricardo A. Mata,[‡] Regine Herbst-Irmer,[†] and Dietmar Stalke*[,†]

[†]Department of Inorganic Chemistry and [‡]Department of Physical Chemistry, Georg-August Universität Göttingen, Tammannstraße 4 and Tammannstraße 6, 37077 Göttingen, Germany

[§]Instituto de Investigaciones en Físico-químicas de Córdoba, Departamento de Química Orgánica, Facultad de Ciencias Químicas, Universidad Nacional de Córdoba, Ciudad Universitaria 5016, Córdoba, Argentina

Supporting Information

ABSTRACT: Pincer complexes of 2,5-bis{(pyrrolidino)-methyl}-pyrrole with group 14 elements such as germanium, tin, and lead were prepared and fully characterized by X-ray single-crystal analysis, NMR spectroscopy, and mass spectrometry. The structures of the complexes were analyzed and compared to the free and the lithiated ligand to gain insight into the effects of metal coordination on the aromatic system. A further aspect was to elaborate the capability of group 14 metals to interact with the pyrrole π-system. Therefore, electronic structure calculations were carried out with group 14 complexes to better understand the bonding situation and the trends among the group. The changes in the aromaticity of the pyrrole ring upon coordination have been rationalized according to the interaction of the π-system with the metal. The unusual short bond distance observed between germanium and the coordinated pyrrole nitrogen was also assessed.

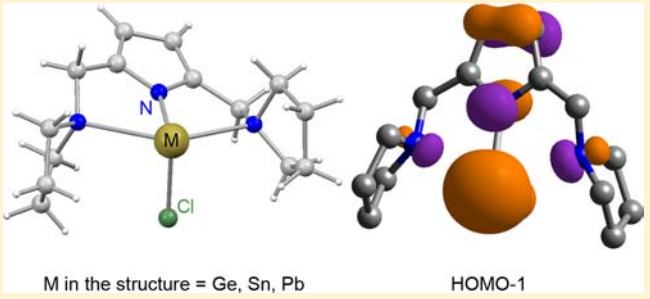

INTRODUCTION

Over the last decades, pincer ligands have played an increasingly important role in coordination chemistry. Reported first by Moulton et al.[1] and van Koten et al.[2] in 1976 and 1978, respectively, they nowadays occupy an increasingly widespread field of application. They are used in inorganic coordination chemistry,[3] as well as in catalysis.[4] This is due to their high degree of flexibility concerning steric and electronic properties, which have been reviewed earlier.[5]

The herein reported pincer ligand consists of three nitrogen donor functions {*NNN*}, which are connected by saturated methylene moieties (Chart 1). Different from our earlier work,[6]

Chart 1. 2,5-Bis{(pyrrolidino)-methyl}pyrrole

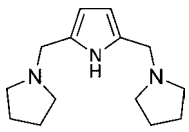

the nitrogen atoms in the side arms display no aromatic character[7] and serve as pure σ-donors, while the central nitrogen atom belongs to a pyrrole-heteroaromatic system. This highly electron-rich π-system interacts strongly with the metal fragments, displayed by short metal−pyrrole bond lengths for all compounds prepared.

Chart 2 shows a simplified orbital diagram for the pyrrole π-system, which will be used to rationalize the effect of metal

Chart 2. Simplified Depiction of the Molecular Orbitals of the Pyrrole π-System

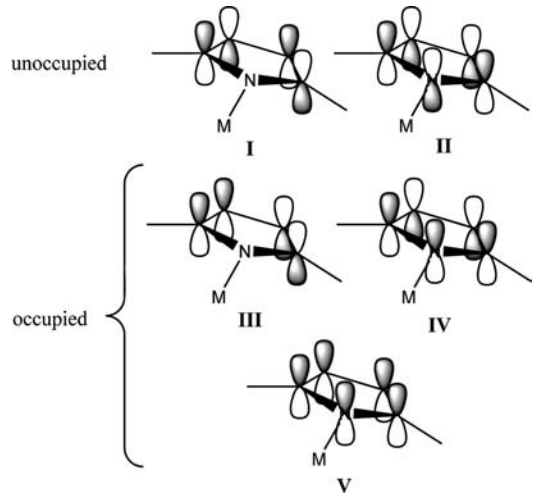

coordination. Molecular orbitals I and III can be neglected because they lack the overlap with the metal ion. In II and IV, it becomes apparent that there are two competing effects. π-Donation from MO IV toward the metal will shorten the C═C double bonds and elongate the C−C single bond, whereas π-

Received: May 16, 2013
Published: July 31, 2013

   dx.doi.org/10.1021/ic401192x | *Inorg. Chem.* 2013, 52, 9539−9548

back-donation from the metal via the lone pair toward the empty pyrrole MO II causes the opposite.[4c] This rather new kind of ligand is perfectly suited to draw inferences from the crystal structure about the metal−ligand interaction of main group metals. However, there is almost no literature present about the detailed investigation of these metal−ligand π-interactions, although these interactions have a substantial influence on the frontier orbitals of the complex and its reactivity. Similar group 14 metal amido species have been reported earlier;[8−10] nevertheless, studying the metal−ligand interactions in detail is considerably hampered in those species because of the rather complicated π-system compared to the π-system of the pyrrole-based pincer ligand reported herein.

Based on the bond lengths inside the heteroaromatic ring, gained from X-ray single-crystal analysis, we will interpret the electronic situation of the π-system and compare it with the results of our theoretical calculations.

RESULTS AND DISCUSSION

The pincer ligand 2,5-bis{(pyrrolidino)methyl}pyrrole (**1**) was prepared following a slightly modified procedure published by Kim et al. in 1998 (Scheme 1).[11]

Scheme 1. Synthesis of 1

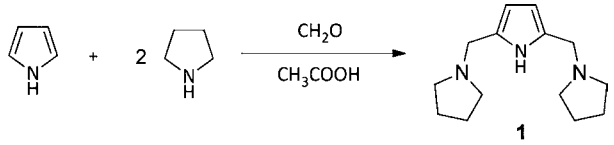

To obtain the metal complexes, **1** was lithiated first either by Li(hmds) or by *n*-butyllithium. Treatment of lithium[2,5-bis{(pyrrolidino)-methyl}-pyrrolide] (**2**) with 1 equiv of the metal halide salt afforded the desired group 14 metal complexes. An increase in yield and purity could be reached by adding **1** to a solution of the metal halides and Li(hmds) (ratio 1:1) (Scheme 2). The free ligand {*NNN*}H (**1**) crystallizes in the orthorhombic space group *Pbca*. The asymmetric unit contains one formula moiety (Figure 1).

Scheme 2. Route to Metal Complexes of 1

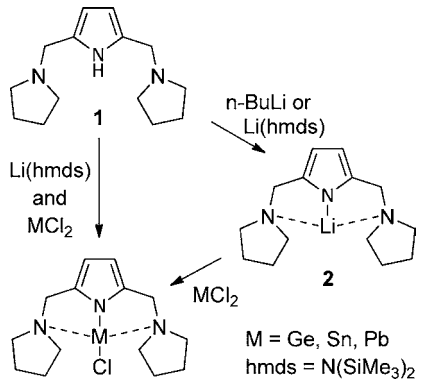

The ligand's shape is determined by the hydrogen bonding pattern. It is formed between H1 and N2′. With a length of 226 pm, the hydrogen bond is considered to be of intermediate strength.[12] In the hydrogen bonding network, it becomes obvious that the ligand molecules are arranged in a linear fashion with the pyrrolidine groups pointing away from the intramolecular NH unit to create sufficient space for dimerization via N2′···H1···N1 intermolecular interaction (Figure 2).

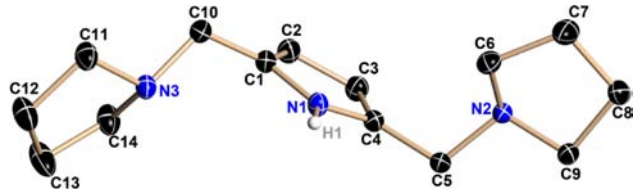

Figure 1. Solid-state structure of {*NNN*}H (**1**). Carbon-bound hydrogen atoms are omitted for clarity. H1 was refined freely, and the anisotropic displacement parameters are depicted at the 50% probability level. Selected bond lengths (pm) and angles (°) C1−C2 137.70(18), C2−C3 141.96(17), C3−C4 137.51(17), N1−H1 85.4(19), N2′···H1 226.0(19), C1−C10−N3 113.95(10), C4−C5−N2 111.94(9), N1−H1···N2′ 163.23.

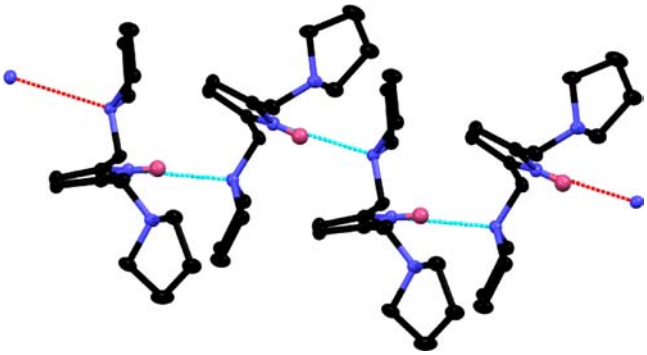

Figure 2. Linear arrangement of **1** via hydrogen bonding.

The heteroaromatic system is planar with the methylene linkers included in that plane. The bond lengths within the pyrrole residue do not differ much from those in free pyrrole, namely, 136 pm for the double bonds and 142 pm for the C−C single bond.[13] The ^{1}H NMR room temperature spectra of **1** show very broad signals for the methylene linkers, as well as for two carbon atoms (C6, C9, C11, C14) in each pyrrolidine moiety, which leads to the assumption that the ligand is not rigid in solution. This can be explained by a flipping-of-the-envelope-like structure of the pyrrolidine. The broadening of the linker signals can be explained by a rotation of the pyrrole-linker bond, which exposes the linker protons to different environments with respect to the heteroaromatic system. This phenomenon is known for that kind of compound and has been described elsewhere.[14]

Group 14 metal complexes (Figure 3) comprise coordination motifs that are very much alike. The metal ion is located in the plane of the heteroaromatic ring, exhibiting a short M−N bond to the pyrrole and longer M−N bonds to the pyrrolidine nitrogen atoms. It is coordinated in a distorted trigonal bipyramidal polyhedron with both pyrrolidine nitrogen atoms at the apical positions and the pyrrole-N, the chloride, and the stereochemically active lone pair in the equatorial positions. The germanium compound (**3**) forms two different N→M donor bonds with pyrrolidine moieties. The radius of germanium(II) is apparently too small compared to the ligands' bite angle, and it is coordinated in an asymmetric fashion. Consequently, the pyrrolidine donor bonds to germanium differ by almost 12 pm. In compound **4**, both metal pyrrolidine

dx.doi.org/10.1021/ic401192x | *Inorg. Chem.* 2013, 52, 9539−9548

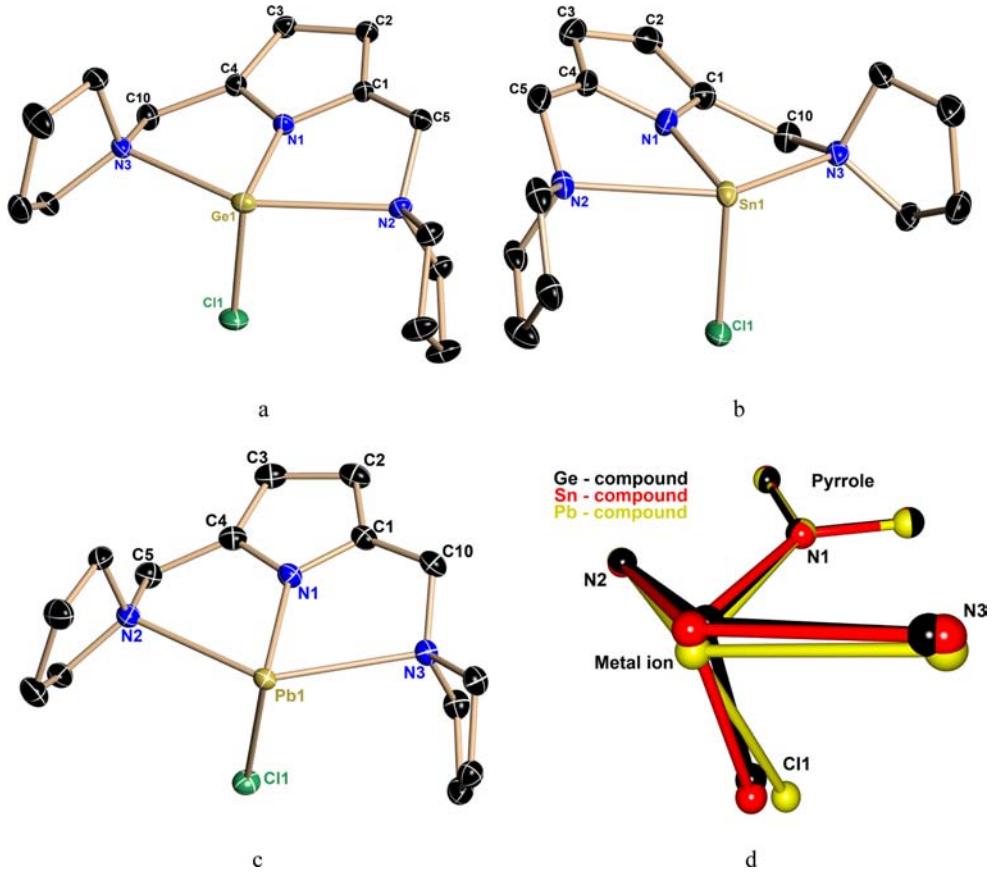

Figure 3. Solid-state structures of group 14 metal complexes of (**3**) (a), (**4**) (b), (**5**) (c) and a superposition plot of all three metal complexes (d). Hydrogen atoms are omitted for clarity. Anisotropic displacement parameters are depicted at the 50% probability level. Selected bond lengths (pm) and angles (°): (a) {*NNN*}GeCl (**3**) N1−Ge1 190.97(7), N2−Ge1 249.75(7), N3−Ge1 238.00(8), C1−C2 137.76(10), C2−C3 143.45(10), C3−C4 137.91(10), N1−Ge1−Cl1 98.49(3), N1−Ge1−N2 73.22(3), N1−Ge1−N3 74.44(3), N2−Ge1−Cl1 93.726(17); (b) {*NNN*}SnCl (**4**) N1−Sn1 211.83(12), N2−Sn1 257.68(12), N3−Sn1 258.56(12), C1−C2 137.8(2), C2−C3 143.0(2), C3−C4 138.1(2), N1−Sn1−Cl1 95.01(4), N1−Sn1−N2 69.22(4), N1−Sn1−N3 69.50(4), N2−Sn1−Cl1 93.97(3); (c) {*NNN*}PbCl (**5**) N1−Pb1 220.00(17), N2−Pb1 261.62(18), N3−Pb1 268.04(19), C1−C2 138.2(3), C2−C3 142.0(3), C3−C4 138.1(3), N1−Pb1−Cl1 90.02(5), N1−Pb1−N2 68.64(6), N1−Pb1−N3 67.46(6), N3−Pb1−Cl1 95.72(4).

bonds are similar because the bigger radius of tin suits the coordination pocket of the ligand better. Similar to **3**, **5** is asymmetric with respect to the N→M donor bonds to pyrrolidine, and the considerably larger lead atom is still coordinated in the {*NNN*} fashion similar to germanium and tin. The reason for the asymmetry is that lead(II) comprises an ion radius larger than the space provided by the ligand in the coordination pocket. This coordination mode seems to be favored in contrast to a symmetrical coordination with both linkers in a rather tensed state.

Compound **3** crystallizes in the tetragonal space group $I\bar{4}$ with a whole molecule in the asymmetric unit. The germanium ion is located in the plane of the heteroaromatic ring, and the Ge−N1 bond is 190.97(7) pm long. Both germanium pyrrolidine bonds are considerably longer by ∼48 and ∼59 pm, respectively. These Ge−N bonds are assumed to be weaker as they are regarded to be donor bonds. An interesting fact is that the C−C−N(2,3) angle at both methylene linkers decreases from ∼111° in **1** to ∼107° in **3**. This decrease is necessary to coordinate smaller and harder ions like germanium(II) in the {*NNN*} fashion and displays the flexibility of the CH_2-linker system. The length of the germanium pyrrole bond of 190.97(7) pm is one of the shortest Ge(II)−N bonds reported in the CSD[15] so far, indicating a strong ligand−metal interaction that includes σ- and π-interactions, as shown in the computational section. Most of the compounds that comprise shorter germanium nitrogen bonds than **3** contain a germanium(IV) atom or show coordination numbers lower than four, resulting in a further bond shortening. The effects of the germanium coordination on the heteroaromatic system are mirrored by the bond lengths of the heteroaromatic ring. With bond lengths of C1−C2 137.76(10), C2−C3 143.45(10), and C3−C4 137.91(10) pm, there are significant changes compared to the free ligand (**1**) (Table 1). The increase in the C2−C3 bond length is counterintuitive for the population of an unoccupied pyrrole-

Table 1. Bond Lengths within the Pyrrole Heteroaromatic Ring and the Average Difference between Single and Double Bonds (Δ_{SB-DB})

	bond lengths			
compound	C1−C2 (pm)	C2−C3 (pm)	C3−C4 (pm)	Δ_{SB-DB} (pm)
{*NNN*}H **1**	137.7	142.0	137.5	4.4
{*NNN*}Ge **3**	137.8	143.5	137.9	5.7
{*NNN*}Sn **4**	137.8	143.0	138.1	5.1
{*NNN*}Pb **5**	138.2	142.0	138.1	3.9

dx.doi.org/10.1021/ic401192x | *Inorg. Chem.* 2013, 52, 9539−9548

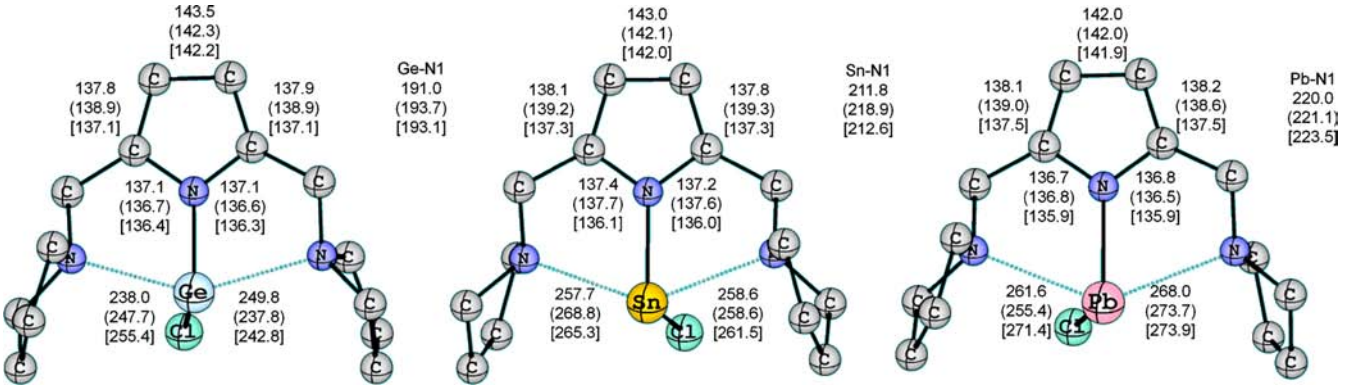

Figure 4. Comparison between the solid state and theoretical structures (M06) [LMP2] of compounds **3**, **4**, and **5**. Selected bond distances are shown in pm. For a clearer reading, the M−N1 distance is given in the top right corner of each compound.

Table 2. MCI (in au), NICS(1)$_{zz}$ and CMO-NICS(1)$_{zz}$ Values (in ppm) for the Free Anion Ligand Compounds 3, 4, and 5. Latter Values Are Shown for the HOMO, HOMO-1, and HOMO-2 Orbitals (See Figure 5)[27]

			CMO-NICS(1)$_{zz}$		
compound	MCI	NICS(1)$_{zz}$	HOMO	HOMO-1	HOMO-2
{*NNN*}$^-$	0.038 (0.038)	−30.2 (−29.8)			
{*NNN*}Ge	0.023 (0.023)	−25.0 (−24.9)	−3.6	+3.6	−2.1
{*NNN*}Sn	0.026 (0.026)	−25.2 (−25.1)	−3.9	−5.2	+7.2
{*NNN*}Pb	0.026 (0.026)	−25.6 (−25.5)	−4.3	−6.2	+9.7

MO by the lone pair of germanium because this would shorten the C2−C3 bond. This elongation can be attributed, however, to the donation of electron density from MO IV (Chart 2) to the germanium ion via π-interaction. Depletion of electron density in MO IV would elongate the C2−C3 bond, which is in good agreement with the observed bond length changes of the free ligand relative to the tetrele metal complexes. Compound **4** crystallizes in the monoclinic space group $P2_1/c$ with one formula moiety in the asymmetric unit. The Sn(II) ion seems to fit perfectly into the bonding pocket of the ligand, which is underlined by two almost identical tin pyrrolidine bonds and almost ideal tetrahedral angles at the linker CH_2 fragments (C1−C10−N3 109.21(11), C4−C5−N2 109.51(11)). With a length of 211.83(12) pm, the N1−Sn1 bond is shorter compared to other Sn(II)−N bonds reported in the CSD,[16] and this is evidence for strong interaction between pyrrole and tin. It can considered a rather strong interaction, although there are shorter tin nitrogen bonds present in the CSD for the same reason already explained when discussing compound **3**. Inspection of the bonding within the pyrrole moiety indicates that π-donation from the heteroaromatic ring toward Sn1 is weaker than in the germanium compound **3**. A consequence of less MO IV metal interaction is a slight decrease in Δ_{SB-DB}, emulating an increase in aromaticity in terms of bond distance equalization. The ^{119}Sn NMR spectrum shows a signal at δ = −217.1 ppm. Unfortunately, there is not even one example in the literature showing a similar four-coordinate motif to the one found in **4**. The reported three-coordinate tin compounds show a similar ^{119}Sn NMR shift range. Starting from δ = −198 ppm ([Sn{N(SiMe$_3$)C(Ph)C(SiMe$_3$)-(C$_5$H$_4$N-2)}Cl])[8e] going to δ = −224 ppm ([HC(CMeNAr)$_2$SnCl], Ar = 2,6-^{i}Pr$_2$C$_6$H$_3$),[8w] δ = −236 ppm ([HC(C^{t}BuNDip)$_2$SnCl], Dip = 2,6-^{i}Pr$_2$C$_6$H$_3$),[10c] up to δ = −281 ppm ([HC(CMeNPh)$_2$SnCl]).[9g] Therefore, the ^{119}Sn NMR signal obtained for **4** can considered to be rather high field shifted.

The lead complex **5** crystallizes in the monoclinic space group $P2_1/c$ with one molecule in the asymmetric unit. The coordination is less strained than expected from an ion radius that large. As it has been already mentioned above, similar to **3**, the lead ion is coordinated in an asymmetrical fashion. The π-system of pyrrole remains almost unaffected compared to the protonated ligand. This could be due to a less pronounced π-interaction or, alternatively, to a counterbalancing effect in the pyrrole metal coordination. The ^{207}Pb NMR spectrum shows a signal at δ = 1524 ppm. For some reason, related structures are published without a ^{207}Pb NMR measurement. There is just one example of a related four-coordinate lead compound containing a ^{207}Pb NMR shift of δ = 1816 ppm ({{2-[(CH$_3$)$_2$NCH$_2$]C$_6$H$_4$}(SiMe$_3$)NPbCl}$_2$).[17]

More detailed information can be obtained from the following electronic structure calculations.

■ COMPUTATIONAL RESULTS

To obtain a deeper insight into the electronic structure and the aromaticity character of the pyrrole moiety in the ligand rather than to judge on distances,[18] electronic structure calculations were carried out on the compounds **3**, **4**, and **5**. Four different methods were used for geometry optimizations, namely, the density functional B3LYP[19] (with and without dispersion corrections)[20] and M06,[21] as well as the local correlated method LMP2.[22] The basis set used was triple-ζ quality (explicated in the Computational Details and will be subsequently referred to as VTZ). Density fitting approximations were used throughout and the "DF-" prefix will be dropped for convenience. All of the methods describe the complexes in good agreement with the X-ray data but with slightly overestimated metal−nitrogen bond lengths (see Figures S1, S2, S3, and Table S1 in the Supporting Information). In this regard, LMP2 and M06 calculations predict the closest geometry to the experimental data. Figure 4 shows the crystal structure values for selected bond distances,

dx.doi.org/10.1021/ic401192x | Inorg. Chem. 2013, 52, 9539−9548

together with M06 and LMP2 results. The LMP2/VTZ root-mean-square deviation values relative to the crystal structures were 15.5, 13.5, and 18.4 pm for compounds **3**, **4**, and **5**, respectively (14.0, 10.6, and 25.7 pm in the case of M06). The asymmetry in the bonding of the pyrrolidine rings to the metal of compound **3** (and to a lesser extent in **5**) is also reproduced. In an attempt to understand the effect of metal coordination on the aromaticity of the pyrrole ring, we have computed two different descriptors of aromaticity based on electron-sharing and magnetic properties, namely, MCI (Multicenter Index)[23] and NICS$(1)_{zz}$ (Nucleus Independent Chemical Shift).[24] Values have been computed for the pyrrole ring in compounds **3**–**5**, and including also the free anion ligand for comparison. The calculations were performed at the M06/VTZ and B3LYP/VTZ levels of theory,[25] and the results are shown in Table 2. Both aromaticity index values are in good agreement with those published for different pyrrole derivatives.[26]

The pincer ligand shows the strongest aromatic character of all the compounds with 0.038 au for MCI and −30.2 ppm from NICS$(1)_{zz}$, which is well within expectations. Upon coordination to the metal, there is a change of roughly 5 ppm in terms of NICS$(1)_{zz}$ values and 0.015 au in terms of the MCI for all compounds studied. In fact, there is little to no change in the NICS$(1)_{zz}$ value when comparing the different metals. There is only a very slight increase in the value in going from Ge to Pb, but given the uncertainty of the method, it would be ill-advised to establish a trend for the metal complexes based on these results.[24b] It is clear that the coordination leads to a decrease in aromaticity, but there is little to no effect in changing the metal within the heavier group 14 series that were considered.

We have also dissected the NICS$(1)_{zz}$ contributions from the highest energy-lying canonical molecular orbitals (CMO-NICS$(1)_{zz}$).[24b,28] As one can observe in Figure 5, these orbitals

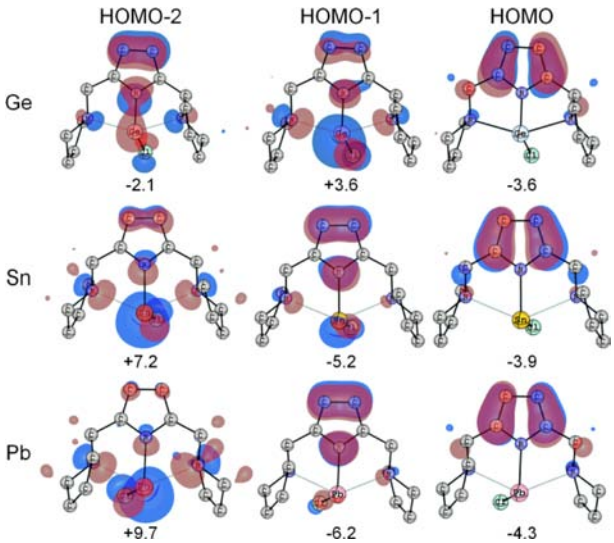

Figure 5. Highest occupied KS molecular orbitals (isocontour 0.045 au) of compounds **3**–**5** (M06/VTZ). The values below each picture represent the canonical molecular contribution to NICS$(1)_{zz}$ results.

correspond to the π-system of the pyrrole ring interacting with the lone pair of M, as well as the bonding orbital between M and the chlorine atoms.[29] One should note that in the case of Ge, the ordering is different from the one observed in Sn and Pb (HOMO-1 and HOMO-2).[10a,30] Two of these orbitals contribute to the aromatic character of the pyrrole ring, and the contribution increases from Ge to Pb. However, the HOMO-2 (HOMO-1 in the case of compound **3**) has a strong antiaromatic contribution, which also increases in about the same magnitude, so that the two effects mostly cancel out. However, one can immediately observe that the two resulting orbitals from the pyrrole MO IV and the M lone pair confirm our previous observations. Going down the group, the interaction decreases gradually (in the case of Pb, the overlap is strongly reduced). In order to better understand the structural patterns observed in this series of compounds, as well as the NICS results, we have applied the Natural Bond Orbital (NBO) method[31] to the three metal group 14 compounds. A particular focus on acceptor−donor interactions has been placed in our analysis. This information together with partial charges and Wiberg bond orders has been included in Table 3. The NBO analysis clearly identifies a bond between the metal and the N1 atom in all cases. The Wiberg bond indices are relatively stable along the series (i.e., 0.456, 0.390, and 0.390 au for complexes **3**, **4**, and **5**, respectively). These values agree with those published for monocationic Ge(II) and Sn(II) systems[32] and are consistent with the description of the cations as being weakly stabilized by donor−acceptor interactions. Interestingly, some clues about the minimal change in the aromaticity character of the pyrrole ring can be also observed from the occupation numbers[33] of the N1 lone pair and C1−C2, as well as C3−C4 bonds (around 1.5 e for the lone pair and 1.8 e for the double bond), together with significant acceptor−donor interactions between the occupied orbitals in the ring and the antibonding C−C orbitals. This falls in agreement with the NICS$(1)_{zz}$ results. Focusing on the metals, little to no change is observed in their charge or the occupation of the metal lone orbital LP(M) when descending the group. The use of partial charges in this context, however, can be somewhat misleading as donation to the pyrrole ring and back-donation can have a balancing effect, together with the interaction of the pyrrolidine nitrogen atoms. To separate these effects, we have applied second-order perturbation theory to compute the NBO acceptor−donor interaction energies $\Delta E^{(2)}$ involving the metal atom. The largest contributions are due to the pyrrolidine nitrogen atoms. These values are given in Table 3. Ge coordinates best with the side arms, but in asymmetric fashion (shorter distance to N3). In the case of Sn, the two nitrogen atoms from the pyrrolidine moieties interact with almost the same energy, in agreement with the symmetry on the distances aforementioned from Figure 3. Compound **5** shows an asymmetric coordination. An interesting point to note is that the energies are, on average, similar to compound **4**.

Because our NBO structure includes an M−N1 covalent bond, the only interaction energies that can be obtained involving the two atoms are a result of delocalization effects. These interaction energies are relatively small compared with the dative interaction discussed above. In this case, the π-donation from the N1 lone pair to the antibonding orbital of the M−Cl bond ($(LPp_z(N_1)\rightarrow\sigma^*(M-Cl))$ (Table 3) amounts to 6.0, 3.7, and 3.6 kcal/mol for Ge, Sn, and Pb complexes, respectively. In a similar way, the π-donation from the N1 lone pair to the metal is even smaller being 1.08, 0.63, and 0.51 kcal/mol for **3**, **4**, and **5**, respectively.

The latter NBO values fall in line with the CMO-NICS$(1)_{zz}$ dissection and the experimental observations. A stronger π-donation lengthens the single bond and shortens the double bonds, leading to an increased separation of the bond

dx.doi.org/10.1021/ic401192x | Inorg. Chem. 2013, 52, 9539−9548

Table 3. NBO Results for Compounds 3, 4, and 5[a]

					$\Delta E^{(2)}$				
compound	Q (M)	LP (M)	LP (N1)	BO (M−N_1)	LPp_z (N_1)→LP* (M)	LPp_z (N_1)→σ* (M−Cl)	LP (N_2)→ LP* (M)	LP (N_3)→LP* (M)	RD (%)
{*NNN*}Ge	+1.042	1.978	1.544	0.456	1.08	6.0	28.9	36.1	1.23
{*NNN*}Sn	+1.190	1.986	1.525	0.390	0.63	3.7	18.9	20.5	1.10
{*NNN*}Pb	+1.190	1.987	1.516	0.390	0.51	3.6	16.5	25.1	0.96

[a]Partial charges (Q, au) and occupation number (LP, au) for the metal atom, Wiberg bond orders (BO, au), percentage of non-Lewis electrons (RD), and second-order acceptor−donor interaction energies ($\Delta E^{(2)}$, kcal/mol) are given. All the calculations were performed at the M06/VTZ level of theory.

distances. The complexation of the ligand with the metal gives a lowering in the aromaticity character.

CONCLUSIONS

We have synthesized group 14 metal complexes (Ge, Sn, and Pb) bearing a pincer ligand based on pyrrole. This π-system is rather convenient to study because of its simplicity and localization within the ligand. Consequently, changes in the pyrrole π-system were traced back to metal−ligand π-interactions and could be studied in detail as these changes could not be compensated for by adjacent π-systems. The observed bond distances change within the pyrrole moiety and hint to a decrease in metal−pyrrole π-interaction, descending group 14. As a result, the degree of aromaticity of the pyrrole ring rises simultaneously. This effect can be explained by a model based on an MO framework, where the pyrrole π-system interacts less favorably with the metal as the metal lone pair increases in energy. Our NBO calculations have shown this trend in detail. Between the metalated compounds, the differences concerning the aromaticity and the occupancy of the metal lone pair are only modest. Remarkably, there is a higher fraction of π-donation from the pyrrole ring to the germanium metal. This explains the unusual short Ge−N distance, while the aromaticity in the ring decreases. The same effect is less pronounced in the tin and lead complexes. The ability for interacting with a π-system increases when ascending group 14. The energy gained by interaction of the pyrrole π-system with germanium is significantly higher than for its heavier analogues, suggesting that the interacting orbitals are more alike in energy than those in **4** and **5**. This is remarkable regarding the aptitude of germanium for catalytic applications where energetically close-lying frontier orbitals are essential.[34] To quantify the π-interaction, however, more investigations with a wide variety of metal species attached to the pyrrole moiety will be conducted.

EXPERIMENTAL SECTION

All experiments were performed under dry argon gas atmosphere by using modified Schlenk techniques or an argon drybox. Solvents were freshly distilled from sodium potassium alloy prior to use. ^{1}H NMR, ^{7}Li,^{13}C, ^{119}Sn, and ^{209}Pb NMR spectra were recorded at room temperature in dry toluene-d_8 using a Bruker Avance III 300 MHz or Bruker DRX 500 MHz spectrometer. All signals were assigned via H,H−COSY and C,H-correlation spectra. EI mass spectra were measured with a MAT 95 instrument. All starting materials were commercially available or synthesized according to the cited literature procedures. Elemental analyses were carried out in the Analytische Labor der Anorganischen Chemie der Universität Göttingen.

Single-Crystal Structural Analysis. Single crystals were selected from a Schlenk flask under argon atmosphere and covered with perfluorated polyether oil on a microscope slide, which was cooled with a nitrogen gas flow using the X-TEMP2 device.[35] An appropriate crystal was selected using a polarizer microscope, mounted on the tip of a MiTeGenMicroMount or glass fiber, fixed to a goniometer head, and shock cooled by the crystal cooling device. The data for **1**, **3**, **4**, and **5** were collected from shock-cooled crystals at 100(2) K. The data sets of **1** and **5** were collected on an Incoatec Mo Microfocus source[36] with mirror optics and APEX II detector with a D8 goniometer. The data set of **3** was measured on a Bruker TXS-Mo rotating anode with mirror optics and APEX II detector with a D8 goniometer. Both diffractometers use Mo Kα radiation (λ = 71.073 pm). The data set of **4** was collected at 100(2) K on SMART APEX Quazar with INCOATEC Ag Microfocus source with mirror optics (Ag Kα, λ = 56.086 pm) and an APEX II detector with a D8 goniometer. The data of **1** and **3**−**5** were integrated with SAINT,[37] and an empirical absorption correction (SADABS)[38] was applied. The structures were solved by direct methods (SHELXS-97) and refined by the full-matrix least-squares method against F^2 (SHELXL-2012)[39] within the SHELXLE-GUI.[40] All non-hydrogen atoms were refined with anisotropic displacement parameters. The C-bound hydrogen atoms were refined isotropically on calculated positions using a riding model with their U_{iso} values constrained equal to 1.5 times the U_{eq} of their pivot atoms for terminal sp^3 carbon atoms and 1.2 times for all other carbon atoms. The N-bound hydrogen atom in **1** was refined freely from the residual density map and constrained to 1.5 U_{eq} of their pivot nitrogen atom. Disordered moieties were refined using bond length restraints and isotropic displacement parameter restraints.[41] Crystallographic data (excluding structure factors) for the structures reported in this paper have been deposited with the Cambridge Crystallographic Data Centre. The CCDC numbers are 928751 (**1**), 928750 (**3**), 928753 (**4**), and 928752 (**5**). Copies of the data can be obtained free of charge from The Cambridge Crystallographic Data Centre via www.ccdc.cam.ac.uk/data_re-quest/cif or from the corresponding author.

Computational Details. All compounds were fully optimized using B3LYP,[19] B3LYP-D3,[20b,42] M06,[21] and LMP2[22] levels of theory. The B3LYP and LMP2 calculations were performed using the MOLPRO 2012.1[43] software program package. The M06 DFT calculations have been performed with the GAUSSIAN 09[44] suite of programs.

Density fitting (DF) approximations have been used in the B3LYP, B3LYP-D3, and local Møller−Plesset perturbation theory calculations.[45] The cc-pVTZ[46] basis set was used for carbon, nitrogen, hydrogen, and chlorine atoms, while for germanium, tin, and lead atoms the Small-Core Dresden/Stuttgart Pseudo Potentials (MDF) 10, 28, and 60 together with def2-TZVPP basis set were used, respectively.[47] In all density fitting calculations reported in this paper, we used the cc-pVTZ/JKJIT and cc-pVTZ/MP2FIT auxiliary fitting basis sets[48] in the HF as well as DFT and LMP2 calculations, respectively. Furthermore, the localized orbitals required for the local correlation methods were generated via the Pipek−Mezey method.[49] The orbitals domains were defined using a NPA criteria T_{NPA} = 0.03.[50] Additionally, analytical Hessians were computed to confirm that the geometries obtained correspond to energetic minima.

For the measure of the aromaticity of the pyrrole rings, we used different indicators. As a magnetic descriptor of aromaticity, we used the Nucleus Independent Chemical Shift (NICS) index, proposed by Schleyer and co-workers.[24a,b] NICS is defined as the negative value of the absolute shielding computed at a ring center or at some other interesting point of the system. Rings with large negative NICS values are considered aromatic. In particular, the gauge-including atomic orbitals (GIAO) method[51] has been used to perform calculations of

dx.doi.org/10.1021/ic401192x | Inorg. Chem. 2013, 52, 9539−9548

NICS ring critical point NICS(0), which is determined by the nonweighted mean of the heavy-atom coordinate and at 1 Å above and below the ring taken into the NICS(1) analysis. It has been postulated that NICS(1) better reflects aromaticity patterns because, at 1 Å, the effects of the π-electron ring current are dominant and local σ-bonding contributions are diminished.[25c,28,52] We have also analyzed the out of plane component of NICS(1), NICS(1)$_{zz}$ which was found to be the best NICS-based indicator of aromaticity.[24c,52] Furthermore, as electronic-based aromaticity descriptor, we have applied the Multicenter Index (MCI).[23] MCI is a particular extension of the I_{ring} index.[24c,53] MCI gives a measure of the electron sharing among all atoms within the ring. The more positive the MCI values, the more aromatic the rings.[25c,26a]

The atomic overlap matrices were generated within Fuzzy-Atom domains with the FUZZY program.[54] Becke's method[55] for multicentric integration with Chebyshev and Lebedev radian and angular quadratures has been used. MCI values were computed at the B3LYP/def2-TVZPP&6-311++G(d,p) level of theory by using the ESI-3D program.[56]

Conjugation interactions have been analyzed in terms of localized molecular orbitals constructed within the Natural Bond Order (NBO)[32] method. The energies associated with the donor−acceptor two-electron interactions have been computed according to the second-order perturbational theory.

General Procedure. For the synthesis of group 14 metal complexes **3**, **4**, and **5**, [LiN(SiMe$_3$)$_2$]·Et$_2$O (1.00 g, 4.14 mmol) was added to a mixture of the group 14 metal halide (4.14 mmol) in toluene (20 mL). The resulting solution was cooled to 0 °C. 2,5-Bis{(pyrrolidino)-methyl}pyrrole (0.97 g, 4.14 mmol) was added, and the solution was stirred for 15 h at room temperature. Filtration of the suspension and reducing the volume of the resulting filtrate yielded crystals suitable for single-crystal X-ray diffraction experiments after storage of the solution at −28 °C for several days.

Bis{(pyrrolidino)-methyl}pyrrole (1). Compound **1** was prepared using a modified protocol published by Kim et al.[11] Pyrrolidine (14.2 g, 200 mmol) was added to glacial acetic acid (12 mL) and cooled to 0 °C. Formaldehyde (37% in MeOH, 15 mL, 200 mmol) was added followed by 10 mL of water. Stirring was continued for 1 h at 0 °C. Then pyrrole (7.2 mL, 100 mmol) was added slowly, and the mixture was allowed to warm up to room temperature. The mixture was then stirred for 18 h at room temperature. Chloroform was added (100 mL), and the pH was adjusted to approximately 10 using aq NaOH (2 M). The organic layer was separated and the solvent removed under reduced pressure. The residue was dissolved in hexane, and the desired compound (15.4 g, 65.9 mmol, 66%) was obtained as colorless crystals after storage for 4 days at −80 °C. ^{1}H NMR (300 MHz): δ (ppm) 9.42 (s$_{br}$, 1 H, pyrrole NH), 6.02 (d, J = 2.6 Hz, 2 H, pyrrole-CH), 3.41 (s, 4 H, 2 linker CH$_2$), 2.37 (m, 8 H, N−CH$_2$ (pyrrolidine)), 1.58 (m, 8 H, N−CH$_2$−*CH*$_2$ (pyrrolidine)). ^{13}C NMR (75 MHz): δ (ppm) 129.7 (pyrrole N−C), 106.7 (pyrrole CH), 54.17 (linker CH$_2$), 53.44 (N−CH$_2$ (pyrrolidine)), 23.89 (N−CH$_2$−CH$_2$ (pyrrolidine)). Anal. Calcd for $C_{14}H_{23}N_3$: C, 72.06; H, 9.93; N, 18.01. Found: C, 71.93; H, 10.12; N, 18.03.

Lithium{2,5-bis{(pyrrolidino)methyl}-pyrrolide} (2). 2,5-Bis-{(pyrrolidino)-methyl}pyrrole (1.00 g, 4.29 mmol) was dissolved in toluene (20 mL) and cooled to 0 °C. A solution of *n*-butyl lithium (*n*-hexane, 6.0 M, 0.71 mL, 4.29 mmol) was added dropwise, and the solution was stirred for 1 h at 0 °C. Subsequently, the ice bath was removed and the solution stirred for 15 h at room temperature. Evaporation of all volatile materials afforded **2** as a white powder (0.92 g, 3.86 mmol, 90%). ^{1}H NMR (300 MHz): δ (ppm) 6.33 (s, 2 H, pyrrole CH), 3.72 (s$_{vbr}$, 4 H, linker CH$_2$), 2.47 (s$_{br}$, 8 H, N−CH$_2$ (pyrrolidine)), 1.40 (m, 8 H, N−CH$_2$−CH$_2$ (pyrrolidine)). ^{13}C NMR (75 MHz): δ (ppm) 138.7 (pyrrole N−C), 105.7 (pyrrole CH), 59.55 (linker CH$_2$), 54.14 (N−CH$_2$ (pyrrolidine)), 23.79 (N−CH$_2$−CH$_2$ (pyrrolidine)). ^{7}Li NMR (117 MHz): δ (ppm) 2.01 (s).

{*NNN*}GeCl (3). Compound **3** was prepared following the general procedure for the synthesis of group 14 metal compounds. The yield was 1.10 g (3.23 mmol, 78% (crystals)). ^{1}H NMR (500 MHz): δ (ppm) 6.09 (s, 2 H, pyrrole CH), 3.67 (d, 2 H, linker CH$_2$), 3.37 (d, 2 H, linker CH$_2$), 2.77 (s$_{br}$, 4 H, N−CH$_2$ (pyrrolidine)), 2.44 (s$_{br}$, 4 H, N−CH$_2$ (pyrrolidine)), 1.57 (m, 8 H, N−CH$_2$−CH$_2$ (pyrrolidine)). ^{13}C NMR (126 MHz): δ (ppm) 132.8 (pyrrole N−C), 104.5 (pyrrole CH), 54.67 (linker CH$_2$), 54.54 (N−CH$_2$ (pyrrolidine)), 23.77 (N−CH$_2$−CH$_2$ (pyrrolidine)). MS (EI): m/z (%) 341 (16), 339 (12), 337 (7), 271 (58), 161 (100), 93 (34), 84 (23). Anal. Calcd for $C_{14}H_{22}ClGeN_3$: C, 49.39; H, 6.51; N, 12.34. Found: C, 49.03; H, 6.67; N, 12.14.

{*NNN*}SnCl (4). Compound **4** was prepared following the general procedure for the synthesis of group 14 metal compounds. The yield was 1.11 g (2.86 mmol, 69% (crystals)). ^{1}H NMR (500 MHz): δ (ppm) 6.13 (s, 2 H, pyrrole CH), 3.65 (d, J = 13.4 Hz, 2 H, linker CH$_2$), 3.39 (d, J = 13.4 Hz, 2 H, linker CH$_2$), 2.34 (s$_{vbr}$, 8 H, N−CH$_2$ (pyrrolidine)), 1.48 (s$_{br}$, 8 H, N−CH$_2$−CH$_2$ (pyrrolidine)). ^{13}C NMR (126 MHz): δ (ppm) 133.5 (pyrrole N−C), 104.8 (pyrrole CH), 55.40 (linker CH$_2$), 54.47 (N−CH$_2$ (pyrrolidine)), 23.69 (N−CH$_2$−CH$_2$ (pyrrolidine)). ^{119}Sn NMR (187 MHz): δ (ppm) −217.1 (s$_{br}$). MS (EI): m/z (%) 389 (7), 387 (19), 385 (14), 317 (60), 161 (100), 93 (15), 84 (18). Anal. Calcd for $C_{14}H_{23}ClN_3Sn$: C, 43.50; H, 5.74; N, 10.87. Found: C, 43.21; H, 5.62; N, 10.87.

{*NNN*}PbCl (5). Compound **5** was prepared following the general procedure for the synthesis of group 14 metal compounds. The yield was 1.06 g (2.24 mmol, 54% (crystals)). ^{1}H NMR (300 MHz): δ (ppm) 6.27 (m, 2 H, pyrrole CH), 3.70 (s$_{br}$, 4 H, linker CH$_2$), 2.55 (s$_{vbr}$, 8 H, N−CH$_2$ (pyrrolidine)), 1.51 (s$_{br}$, 8 H, N−CH$_2$−CH$_2$ (pyrrolidine)). ^{13}C NMR (126 MHz): δ (ppm) 138.3 (pyrrole N−C), 105.7 (pyrrole CH), 56.61 (linker CH$_2$), 54.32 (N−CH$_2$ (pyrrolidine)), 23.75 (N−CH$_2$−CH$_2$ (pyrrolidine)). ^{207}Pb NMR (63 MHz): δ (ppm) 1524 (m). MS (EI): m/z (%) 475 (16), 474 (7), 473(7), 405 (44), 161 (100), 93(23), 84 (19). Anal. Calcd for $C_{14}H_{23}ClN_3Pb$: C, 35.40; H, 4.67; N, 8.85. Found: C, 35.31; H, 4.38; N, 9.15.

■ ASSOCIATED CONTENT

Supporting Information

Further experimental and theoretical details, physical and spectroscopic data for **1** and **3**−**5** and CIF data, as well as from theory. This material is available free of charge via the Internet at http://pubs.acs.org.

■ AUTHOR INFORMATION

Corresponding Author

*E-mail: dstalke@chemie.uni-goettingen.de.

Notes

The authors declare no competing financial interest.

■ ACKNOWLEDGMENTS

We thank the Danish National Research Foundation (DNRF93), which funded the *Center for Materials Crystallography* (CMC), for partially supporting this research project and the Land Niedersachsen for providing a Lichtenberg fellowship in the Catalysis for Sustainable Synthesis (CaSuS) Ph.D. Program. D.M.A. gratefully acknowledges a postdoctoral fellowship from ARCOIRIS Erasmus Mundus Action 2. The authors thank Professor Miquel Solà (Universitat de Girona, Campus de Montilivi, Girona, Spain) for providing computational time in software and hardware. All the assistance and helpful comments from Dr. Eduard Matito and Dr. Pedro Salvador are greatly acknowledged.

■ REFERENCES

(1) Moulton, C. J.; Shaw, B. L. *J. Chem. Soc., Dalton Trans.* **1976**, 1020−1024.

(2) van Koten, G.; Jastrzebski, J. T. B. H.; Noltes, J. G.; Spek, A. L.; Schoone, J. C. *J. Organomet. Chem.* **1978**, *148*, 233−245.

(3) (a) Khan, S.; Michel, R.; Dieterich, J. M.; Mata, R. A.; Roesky, H. W.; Demers, J.-P.; Lange, A.; Stalke, D. *J. Am. Chem. Soc.* **2011**, *133*,

17889−17894. (b) Jentner, J.; Gamer, M. T.; Roesky, P. W. *Organometallics* **2010**, *29*, 4410−4413. (c) Jenter, J.; Roesky, P. W. *New J. Chem.* **2010**, *34*, 1541−1543. (d) Khan, S.; Samuel, P. P.; Michel, R.; Dieterich, J. M.; Mata, R. A.; Demers, J.-P.; Lange, A.; Roesky, H. W.; Stalke, D. *Chem. Commun.* **2012**, *48*, 4890−4892. (e) Lien, Y.-L.; Chang, Y.-C.; Chuang, N.-T.; Datta, A.; Chen, S.-J.; Hu, C.-H.; Huang, W.-Y.; Lin, C.-H.; Huang, J.-H. *Inorg. Chem.* **2010**, *49*, 136−143.

(4) (a) Mazet, C.; Gade, L. H. *Chem.—Eur. J.* **2003**, *9*, 1759−1767. (b) Kumar, S.; Mani, G.; Mondal, S.; Chattaraj, P.-K. *Inorg. Chem.* **2012**, *51*, 12527−12539. (c) Imler, G. H.; Lu, Z.; Kistler, K. A.; Carroll, P. J.; Wayland, B. B.; Zdilla, M. J. *Inorg. Chem.* **2012**, *51*, 10122−10128. (d) Grüger, N.; Wadepohl, H.; Gade, L. H. *Dalton Trans.* **2012**, *41*, 14028−14030. (e) Denney, M. C.; Pons, V.; Hebden, T. J.; Heinekey, D. M.; Goldberg, K. I. *J. Am. Chem. Soc.* **2006**, *128*, 12048−12049. (f) Goldman, A. S.; Roy, A. H.; Huang, Z.; Ahuja, R.; Schinski, W.; Brookhart, M. *Science* **2006**, *312*, 257−261. (g) Zhao, J.; Goldman, A. S.; Hartwig, J. F. *Science* **2005**, *307*, 1080−1082. (h) Kohl, S. W.; Weiner, L.; Swartsburd, L.; Kostanikowski, L.; Shimon, L. J. W.; Ben-David, Y.; Iron, M. A.; Milstein, D. *Science* **2009**, *324*, 74−77. (i) Hahn, F. E.; Jahnke, M. C.; Gomez-Benitez, V.; Morales-Morales, D.; Pape, T. *Organometallics* **2005**, *24*, 6458−6463. (j) Khaskin, E.; Iron, M. A.; Shimon, L. J. W.; Zhang, J.; Milstein, D. *J. Am. Chem. Soc.* **2010**, *132*, 8542−8543. (k) Balaraman, E.; Gunanathan, C.; Zhang, J.; Shimon, L. J. W.; Milstein, D. *Nat. Chem.* **2011**, *3*, 609−614. (l) Tian, R.; Ng, Y.; Ganguly, R.; Mathey, F. *Organometallics* **2012**, *31*, 2486−2488. (m) Friedrich, A.; Drees, M.; Käss, M.; Herdtweck, E.; Schneider, S. *Inorg. Chem.* **2010**, *49*, 5482−5494. (n) Askevold, B.; Nieto, J. T.; Tussupbayev, S.; Diefenbach, M.; Herdtweck, E.; Holthausen, M. C.; Schneider, S. *Nat. Chem.* **2011**, *3*, 532−537. (o) Askevold, B.; Roesky, H. W.; Schneider, S. *ChemCatChem* **2012**, *4*, 307−320. (p) Scheibel, M. G.; Askevold, B.; Heinemann, F. W.; Reijerse, E. J.; de Bruin, B.; Schneider, S. *Nat. Chem.* **2012**, *4*, 552−558. (q) de Boer, S. Y.; Gloaguen, Y.; Reek, J. N. H.; Lutz, M.; van der Vlugt, J. I. *Dalton Trans.* **2012**, *41*, 11276−11283. (r) Löble, M. W.; Casimiro, M.; Thielemann, D. T.; Ona-Burgos, P.; Fernandez, I.; Roesky, P. W.; Breher, F. *Chem.—Eur. J.* **2012**, *18*, 5325−5334.

(5) (a) Schneider, S.; Meiners, J.; Askevold, B. *Eur. J. Inorg. Chem.* **2012**, 412−429. (b) Albrecht, M.; Lindner, M. M. *Dalton Trans.* **2011**, *40*, 8733−9744. (c) Albrecht, M.; van Koten, G. *Angew. Chem., Int. Ed.* **2001**, *40*, 3750−3781. (d) Pugh, D.; Danopoulos, A. A. *Coord. Chem. Rev.* **2007**, *251*, 610−641. (e) van der Boom, M. E.; Milstein, D. *Chem. Rev.* **2003**, *103*, 1759−1792.

(6) (a) Gornitzka, H.; Stalke, D. *Eur. J. Inorg. Chem.* **1998**, 311−317. (b) Pfeiffer, M.; Baier, F.; Stey, T.; Stalke, D.; Engels, B.; Moigno, D.; Kiefer, W. *J. Mol. Model.* **2000**, *6*, 299−311. (c) Pfeiffer, M.; Murso, A.; Mahalakshmi, L.; Moigno, D.; Kiefer, W.; Stalke, D. *Eur. J. Inorg. Chem.* **2002**, 3222−3234.

(7) Fauré, J.-L.; Gornitzka, H.; Réau, R.; Stalke, D.; Bertrand, G. *Eur. J. Inorg. Chem.* **1999**, 2295−2299.

(8) (a) Jones, C.; Bonyhady, S. J.; Holzmann, N.; Frenking, G.; Stasch, A. *Inorg. Chem.* **2011**, *50*, 12315−12325. (b) Matioszek, D.; Kafir, N.; Saffon, N.; Castel, A. *Organometallics* **2010**, *29*, 3039−3046. (c) Chlupaty, T.; Padelkova, Z.; Lycka, A.; Bruns, J.; Ruzicka, A. *Dalton Trans.* **2012**, *41*, 5010−5019. (d) Fedushkin, I. L.; Khvoinova, N. M. *Inorg. Chem.* **2004**, *43*, 7807−7815. (e) Leung, W.-P.; So, C.-W.; Wu, Y.-S.; Li, H.-W.; Mak, T. C. W. *Eur. J. Inorg. Chem.* **2005**, 513−521. (f) Arii, H.; Nakadate, F.; Mochida, K.; Kawashima, T. *Organometallics* **2011**, *30*, 4471−4474. (g) Chrostowska, A.; Lemierre, V.; Pigot, T.; Pfister-Guillouzo, G.; Saur, I.; Miqueu, K.; Rima, G.; Barrau, J. *Main Group Met. Chem.* **2002**, *25*, 469−474. (h) Fedushkin, I. L.; Hummert, M.; Schumann, H. *Eur. J. Inorg. Chem.* **2006**, 3266−3273. (i) Jones, C.; Rose, R. P.; Stasch, A. *Dalton Trans.* **2008**, 2871−2878. (j) Wang, W.; Inoue, S.; Yao, S.; Driess, M. *Organometallics* **2011**, *30*, 6490−6494. (k) Reddy, N. D.; Jana, A.; Roesky, H. W.; Samuel, P. P.; Schulzke, C. *Dalton Trans.* **2010**, *39*, 234−238. (l) Woodul, W. D.; Richards, A. F.; Stasch, A.; Driess, M.; Jones, C. *Organometallics* **2010**, *29*, 3655−3660. (m) Sarish, S. P.; Sen, S. S.; Roesky, H. W.; Objartel, I.; Stalke, D. *Chem. Commun.* **2011**, *47*, 7206−7208. (n) Siwatch, R. K.; Kundu, S.; Kumar, D.; Nagendran, S. *Organometallics* **2011**, *30*, 1998−2005. (o) Ayers, A. E.; Klapotke, T. M.; Dias, H. V. R. *Inorg. Chem.* **2001**, *40*, 1000−1005. (p) Vasudevan, K. V.; Vargas-Baca, J.; Cowley, A. H. *Angew. Chem., Int. Ed.* **2009**, *48*, 8369−8371. (q) Green, S. P.; Jones, C.; Junk, P. C.; Lippert, K.-A.; Stasch, A. *Chem. Commun.* **2006**, 3978−3980. (r) Dias, H. V.; Wang, Z. *J. Am. Chem. Soc.* **1997**, *119*, 4650−4655. (s) Filippou, A. C.; Portius, P.; Kociok-Kohn, G. *Chem. Commun.* **1998**, 2327−2328. (t) Nagendran, S.; Sen, S. S.; Roesky, H. W.; Koley, D.; Grubmüller, H.; Pal, A.; Herbst-Irmer, R. *Organometallics* **2008**, *27*, 5459−5463. (u) Ayers, A. E.; Dias, H. V. R. *Inorg. Chem.* **2002**, *41*, 3259−3268. (v) Gushwa, A. F.; Richards, A. F. *J. Chem. Cryst.* **2006**, *36*, 851−856. (w) Ding, Y.; Roesky, H. W.; Noltemeyer, M.; Schmidt, H.-G.; Power, P. P. *Organometallics* **2001**, *20*, 1190−1194. (x) Yang, Z.; Ma, X.; Roesky, H. W.; Yang, Y.; Zhu, H.; Magull, J.; Ringe, A. *Z. Anorg. Allg. Chem.* **2008**, *634*, 1490−1492.

(9) (a) Cowley, A. H.; Geerts, R. L.; Nurm, C. M.; Carrano, C. J. *J. Organomet. Chem.* **1988**, *341*, C27−C30. (b) Doyle, D. J.; Hitchcock, P. B.; Lappert, M. F.; Li, G. *J. Organomet. Chem.* **2009**, *694*, 2611−2617. (c) Sen, S. S.; Kritzler-Kosch, M. P.; Nagendran, S.; Roesky, H. W.; Beck, T.; Pal, A.; Herbst-Irmer, R. *Eur. J. Inorg. Chem.* **2010**, 5304−5311. (d) Ferro, L.; Hitchcock, P. B.; Coles, M. P.; Cox, H.; Futton, J. R. *Inorg. Chem.* **2011**, *50*, 1879−1888. (e) Reger, D. L.; Knox, S. J.; Huff, M. F.; Rheingold, A. L.; Haggerty, B. J. *Inorg. Chem.* **1991**, *30*, 1754−1759. (f) Hitchcock, P. B.; Hu, J.; Lappert, M. F.; Severn, J. R. *Dalton Trans.* **2004**, 4193−4201. (g) Akkari, A.; Byrne, J. J.; Saur, I.; Rima, G.; Gornitzka, H.; Barrau, J. *J. Organomet. Chem.* **2001**, *622*, 190−198. (h) Bryn, M.; Francis, M. D.; Jin, G.; Jones, C.; Mills, D. P.; Stasch, A. *Organometallics* **2006**, *25*, 4799−4807. (i) Kobayasi, J.; Kushida, T.; Kawashima, T. *J. Am. Chem. Soc.* **2009**, *131*, 10836−10837. (j) Dias, H. V. R.; Jin, W. *J. Am. Chem. Soc.* **1996**, *118*, 9123−9126. (k) Jastrzebski, J. T. B. H.; van der Schaaf, P. A.; Boersma, J.; van Koten, G.; Zoutberg, M. C.; Heijdenrijk, D. *Organometallics* **1989**, *8*, 1373−1375. (l) Nimitsiriwat, N.; Gibson, V. C.; Marshall, E. L.; With, A. J. P.; Dale, S. H.; Elsegood, N. R. J. *Dalton Trans.* **2007**, 4464−4471.

(10) (a) Chen, M.; Fulton, J. R.; Hitchcock, P. B.; Johnstone, N. C.; Lappert, M. F.; Protchenko, A. V. *Dalton Trans.* **2007**, 2770−2778. (b) Stasch, A.; Forsyth, C. M.; Jones, C.; Junk, P. C. *New J. Chem.* **2008**, *32*, 829−834. (c) Choong, S. L.; Schenk, C.; Stasch, A.; Dange, D.; Jones, C. *Chem. Commun.* **2012**, *48*, 2504−2506.

(11) Kim, I. T.; Elsenbaumer, R. L. *Tetrahedron Lett.* **1998**, *39*, 1087−1090.

(12) (a) Desiraju, G. R. *Angew. Chem., Int. Ed. Engl.* **1995**, *34*, 2311−2327. (b) Desiraju, G. R.; Steiner, T. *The Weak Hydrogen Bond in Structural Chemistry and Biology*; Oxford University Press: Oxford, UK, 1999. (c) Steiner, T. *Angew. Chem.* **2002**, *114*, 50−80. (d) Steiner, T. *Angew. Chem., Int. Ed.* **2002**, *41*, 48−76.

(13) Goddard, R.; Heinemann, O.; Krüger, C. *Acta Crystallogr., Sect. C: Cryst. Struct. Commun.* **1997**, *53*, 1846−1850.

(14) (a) Kuo, P.-C.; Chang, J.-C.; Lee, W.-Y.; Lee, H. M.; Huang, J.-H. *J. Organomet. Chem.* **2005**, *690*, 4168−4174. (b) Ghorai, D.; Kumar, S.; Mani, G. *Dalton Trans.* **2012**, *41*, 9503−9512.

(15) *Cambridge Crystal Structure Database* search for Ge−N bond lengths yielded 2160 entries with a mean value of 197.1 pm. The minimum bond length is 172.6 pm and the longest Ge−N bond is 273.8 pm long.

(16) *Cambridge Crystal Structure Database* search for Sn−N bond lengths yielded 6426 entries with a mean value of 227.9 pm. The minimum bond length is 189.9 pm and the longest Sn−N bond is 322.1 pm long.

(17) Vankatova, H.; Broeckaert, L.; De Proft, F.; Olejnik, R.; Turek, J.; Padelkova, Z.; Ruzicka, A. *Inorg. Chem.* **2011**, *50*, 9454−9464.

(18) (a) Kaupp, M.; Metz, B.; Stoll, H. *Angew. Chem., Int. Ed.* **2000**, *39*, 4607. (b) Kaupp, M.; Metz, B.; Stoll, H. *Angew. Chem.* **2000**, *112*, 4780.

(19) (a) Becke, A. D. *J. Chem. Phys.* **1993**, *98*, 5648−5652. (b) Lee, C.; Yang, W.; Parr, R. G. *Phys. Rev. B* **1988**, *37*, 785−789. (c) Stephens,

P. J.; Devlin, F. J.; Chabalowski, C. F.; Frisch, M. J. *J. Phys. Chem.* **1994**, *98*, 11623−11627. (d) Becke, A. D. *Phys. Rev. A* **1988**, *38*, 3098−3100.
(20) (a) Grimme, S. *J. Comput. Chem.* **2004**, *25*, 1463−1473. (b) Grimme, S. *J. Comput. Chem.* **2006**, *27*, 1787−1799.
(21) Zhao, Y.; Truhlar, D. G. *Theor. Chem. Acc.* **2008**, *120*, 215−241.
(22) (a) Hetzer, G.; Pulay, P.; Werner, H. J. *Chem. Phys. Lett.* **1998**, *290*, 143−149. (b) Pulay, P. *Chem. Phys. Lett.* **1983**, *100*, 151−154. (c) Sæbø, S.; Pulay, P. *Chem. Phys. Lett.* **1985**, *113*, 13−18. (d) Hetzer, G.; Schütz, M.; Stoll, H.; Werner, H. J. *J. Chem. Phys.* **2000**, *113*, 9443. (e) Saebø, S.; Pulay, P. *J. Chem. Phys.* **1988**, *88*, 1884. (f) Saebø, S.; Pulay, P. *J. Chem. Phys.* **1987**, *86*, 914. (g) Schütz, M.; Hetzer, G.; Werner, H. J. *J. Chem. Phys.* **1999**, *111*, 5691. (h) Rauhut, G.; Pulay, P.; Werner, H. J. *J. Comput. Chem.* **1998**, *19*, 1241−1254. (i) Pulay, P.; Saebø, S. *Theor. Chim. Acta* **1986**, *69*, 357−368.
(23) (a) Bultinck, P.; Ponec, R.; Van Damme, S. *J. Phys. Org. Chem.* **2005**, *18*, 706−718. (b) Bultinck, P.; Fias, S.; Ponec, R. *Chem.—Eur. J.* **2006**, *12*, 8813−8818. (c) Bultinck, P.; Rafat, M.; Ponec, R.; Van Gheluwe, B.; Carbó-Dorca, R.; Popelier, P. *J. Phys. Chem. A* **2006**, *110*, 7642−7648.
(24) (a) Schleyer, P. V. R.; Maerker, C.; Dransfeld, A.; Jiao, H.; van Eikema Hommes, N. J. R. *J. Am. Chem. Soc.* **1996**, *118*, 6317−6318. (b) Chen, Z.; Wannere, C. S.; Corminboeuf, C.; Puchta, R.; Schleyer, P. V. R. *Chem. Rev.* **2005**, *105*, 3842−3888. (c) Fallah-Bagher-Shaidaei, H.; Wannere, C. S.; Corminboeuf, C.; Puchta, R.; Schleyer, P. V. R. *Org. Lett.* **2006**, *8*, 863−866.
(25) (a) Badri, Z.; Foroutan-Nejad, C.; Rashidi-Ranjbar, P. *Phys. Chem. Chem. Phys.* **2012**, *14*, 3471−3481. (b) Feixas, F.; Matito, E.; Poater, J.; Solà, M. *J. Comput. Chem.* **2008**, *29*, 1543−1554. (c) Solà, M.; Feixas, F.; Jiménez-Halla, J. O. C.; Matito, E.; Poater, J. *Symmetry* **2010**, *2*, 1156−1179.
(26) (a) Feixas, F.; Jiménez-Halla, J. O. C.; Matito, E.; Poater, J.; Solà, M. *J. Chem. Theory Comput.* **2010**, *6*, 1118−1130. (b) Curutchet, C.; Poater, J.; Solà, M.; Elguero, J. *J. Phys. Chem. A* **2011**, *115*, 8571−8577. (c) Blanco, F.; Alkorta, I.; Zborowski, K.; Elguero, J. *Struct. Chem.* **2007**, *18*, 965−975. (d) Zborowski, K.; Alkorta, I.; Elguero, J. *Struct. Chem.* **2007**, *18*, 797−805.
(27) (a) All the values were computed at M06/VTZ//LMP2/VTZ and B3LYP/VTZ//LMP2/VTZ (in parentheses). (b) Each value is the average between NICS(1)$_{zz}$ values of both faces above and below the plane of the ring. (c) MCI calculations were performed using the wavefunctions at M06/def2-TVZPP&6-311++G(d,p)//LMP2/VTZ and B3LYP/def2-TVZPP&6-311++G(d,p)//LMP2/VTZ (in parentheses).
(28) Schleyer, P. V. R.; Manoharan, M.; Wang, Z. X.; Kiran, B.; Jiao, H.; Puchta, R.; van Eikema Hommes, N. J. *Org. Lett.* **2001**, *3*, 2465−2468.
(29) Henn, M.; Deáky, V.; Krabbe, S.; Schürmann, M.; Prosenc, M. H.; Herres-Pawlis, S.; Mahieu, B.; Jurkschat, K. *Z. Anorg. Allg. Chem.* **2011**, *637*, 211−223.
(30) Ullah, F.; Bajor, G.; Veszpremi, T.; Jones, P. G.; Heinicke, J. W. *Angew. Chem., Int. Ed.* **2007**, *46*, 2697.
(31) (a) Reed, A. E.; Weinhold, F. *J. Chem. Phys.* **1983**, *78*, 4066−4073. (b) Reed, A. E.; Weinhold, F. *J. Chem. Phys.* **1985**, *83*, 1736−1740. (c) Reed, A. E.; Curtiss, L. A.; Weinhold, F. *Chem. Rev.* **1988**, *88*, 899−926. (d) Reed, A. E.; Weinstock, R. B.; Weinhold, F. *J. Chem. Phys.* **1985**, *83*, 735−746.
(32) (a) Xiong, Y.; Yao, S.; Inoue, S.; Berkefeld, A.; Driess, M. *Chem. Commun.* **2012**, *48*, 12198−12200. (b) Li, J.; Schenk, C.; Winter, F.; Scherer, H.; Trapp, N.; Higelin, A.; Keller, S.; Pöttgen, R.; Krossing, I.; Jones, C. *Angew. Chem., Int. Ed.* **2012**, *51*, 9557−9561.
(33) Mazurek, A.; Dobrowolski, J. C. *J. Org. Chem.* **2012**, *77*, 2608−2618.
(34) Power, P. P. *Nature* **2010**, *463*, 171−177.
(35) (a) Kottke, T.; Stalke, D. *J. Appl. Crystallogr.* **1993**, *26*, 615−619. (b) Kottke, T.; Lagow, R. J.; Stalke, D. *J. Appl. Crystallogr.* **1996**, *29*, 465−468. (c) Stalke, D. *Chem. Soc. Rev.* **1998**, *27*, 171−178.
(36) Schulz, T.; Meindl, K.; Leusser, D.; Stern, D.; Graf, J.; Michaelsen, C.; Ruf, M.; Sheldrick, G. M.; Stalke, D. *J. Appl. Crystallogr.* **2009**, *42*, 885−891.
(37) *SAINT v7.68A in Bruker APEX2 v2012.2-0*, Bruker AXS Inst., Inc.: Madison, WI, USA, 2012.
(38) Sheldrick, G. M. *SADABS-2012/1*; Universität Göttingen: Göttingen, Germany, 2012.
(39) Sheldrick, G. M. *Acta Crystallogr., Sect. A* **2008**, *64*, 112−122.
(40) Huebschle, C. B.; Sheldrick, G. M.; Dittrich, B. *J. Appl. Crystallogr.* **2011**, *44*, 1281−1284.
(41) Müller, P.; Herbst-Irmer, R.; Spek, A. L.; Schneider, T. R.; Sawaya, M. R. In *Crystal Structure Refinement—A Crystallographer's Guide to SHELXL, IUCr Texts on Crystallography*; Müller, P., Ed.; Oxford University Press: Oxford, UK, 2006; Vol. *8*.
(42) (a) Schwabe, T.; Grimme, S. *Acc. Chem. Res.* **2008**, *41*, 569−579. (b) Grimme, S.; Antony, J.; Ehrlich, S.; Krieg, H. *J. Chem. Phys.* **2010**, *132*, 154104.
(43) (a) Werner, H.-J.; Knowles, P. J.; Knizia, G.; Manby, F. R.; Schütz, M. *Wiley Interdiscip. Rev.: Comput. Mol. Sci.* **2012**, *2*, 242−253. (b) Werner, H.-J.; Knowles, P. J.; Knizia, G.; Manby, F. R.; Schütz, M.; Celani, P.; Korona, T.; Lindh, R.; Mitrushenkov, A.; Rauhut, G.; Shamasundar, K. R.; Adler, T. B.; Amos, R. D.; Bernhardsson, A.; Berning, A.; Cooper, D. L.; Deegan, M. J. O.; Dobbyn, A. J.; Eckert, F.; Goll, E.; Hampel, C.; Hesselmann, A.; Hetzer, G.; Hrenar, T.; Jansen, G.; Köppl, C.; Liu, Y.; Lloyd, A. W.; Mata, R. A.; May, A. J.; McNicholas, S. J.; Meyer, W.; Mura, M. E.; Nicklass, A.; O'Neill, D. P.; Palmieri, P.; Peng, D.; Pflüger, K.; Pitzer, R.; Reiher, M.; Shiozaki, T.; Stoll, H.; Stone, A. J.; Tarroni, R.; Thorsteinsson, T.; Wang, M. http://www.molpro.net, 2012.
(44) Frisch, M. J.; Trucks, G. W.; Schlegel, H. B.; Scuseria, G. E.; Robb, M. A.; Cheeseman, J. R.; Scalmani, G.; Barone, V.; Mennucci, B.; Petersson, G. A.; Nakatsuji, H.; Caricato, M.; Li, X.; Hratchian, H. P.; Izmaylov, A. F.; Bloino, J.; Zheng, G.; Sonnenberg, J. L.; Hada, M.; Ehara, M.; Toyota, K.; Fukuda, R.; Hasegawa, J.; Ishida, M.; Nakajima, T.; Honda, Y.; Kitao, O.; Nakai, H.; Vreven, T.; Montgomery, J. A., Jr.; Peralta, J. E.; Ogliaro, F.; Bearpark, M.; Heyd, J. J.; Brothers, E.; Kudin, K. N.; Staroverov, V. N.; Kobayashi, R.; Normand, J.; Raghavachari, K.; Rendell, A.; Burant, J. C.; Iyengar, S. S.; Tomasi, J.; Cossi, M.; Rega, N.; Millam, J. M.; Klene, M.; Knox, J. E.; Cross, J. B.; Bakken, V.; Adamo, C.; Jaramillo, J.; Gomperts, R.; Stratmann, R. E.; Yazyev, O.; Austin, A. J.; Cammi, R.; Pomelli, C.; Ochterski, J. W.; Martin, R. L.; Morokuma, K.; Zakrzewski, V. G.; Voth, G. A.; Salvador, P.; Dannenberg, J. J.; Dapprich, S.; Daniels, A. D.; Farkas, O.; Foresman, J. B.; Ortiz, J. V.; Cioslowski, J.; Fox, D. J. *Gaussian 09*, revision A.02; Gaussian, Inc.: Wallingford, CT, 2010.
(45) (a) Schütz, M.; Werner, H. J.; Lindh, R.; Manby, F. R. *J. Chem. Phys.* **2004**, *121*, 737. (b) Werner, H. J.; Manby, F. R.; Knowles, P. J. *J. Chem. Phys.* **2003**, *118*, 8149. (c) Polly, R.; Werner, H. J.; Manby, F. R.; Knowles, P. J. *Mol. Phys.* **2004**, *102*, 2311−2321.
(46) (a) Dunning, T. H., Jr. *J. Chem. Phys.* **1989**, *90*, 1007. (b) Woon, D. E.; Dunning, T. H., Jr. *J. Chem. Phys.* **1993**, *98*, 1358.
(47) (a) Weigend, F.; Ahlrichs, R. *Phys. Chem. Chem. Phys.* **2005**, *7*, 3297−3305. (b) Metz, B.; Stoll, H.; Dolg, M. *J. Chem. Phys.* **2000**, *113*, 2563.
(48) (a) Weigend, F.; Köhn, A.; Hättig, C. *J. Chem. Phys.* **2002**, *116*, 3175. (b) Hättig, C. *Phys. Chem. Chem. Phys.* **2005**, *7*, 59−66. (c) Weigend, F. *Phys. Chem. Chem. Phys.* **2002**, *4*, 4285−4291.
(49) Pipek, J.; Mezey, P. G. *J. Chem. Phys.* **1989**, *90*, 4916.
(50) Mata, R. A; Werner, M. J. *Mol. Phys.* **2007**, *105*, 2753−2761.
(51) Wolinski, K.; Hinton, J. F.; Pulay, P. *J. Am. Chem. Soc.* **1990**, *112*, 8251−8260.
(52) Corminboeuf, C.; Heine, T.; Seifert, G.; Schleyer, P. V. R.; Weber, J. *Phys. Chem. Chem. Phys.* **2004**, *6*, 273−276.
(53) (a) Giambiagi, M.; de Giambiagi, M. S.; dos Santos Silva, C. D.; de Figueiredo, A. P. *Phys. Chem. Chem. Phys.* **2000**, *2*, 3381−3392. (b) Cioslowski, J.; Matito, E.; Solà, M. *J. Phys. Chem. A* **2007**, *111*, 6521−6525.
(54) Mayer, I.; Salvador, P. FUZZY, version 1.00; Girona, Spain, 2003.

(55) Becke, A. D. *J. Chem. Phys.* **1988**, *88*, 2547.
(56) Matito, E. ESI-3D: Electron Sharing Indexes Program for 3D Molecular Space Partitioning; Institute of Computational Chemistry: Girona, Spain, 2006, http//:iqc.udg.edu/eduard/ESI.